Powders and Grains (2005) – García-Rojo, Herrmann and McNamara (eds)

Relating particle characteristics to macro behavior of DEM crushable material

Y. Nakata
Yamaguchi University, Japan

M.D. Bolton & Y.P. Cheng
Cambridge University, UK

ABSTRACT: The behavior of a real soil is influenced by the crushing strength of its grains as well as their contact stiffness and coefficient of friction. This can conveniently be explored by DEM, creating agglomerates of bonded micro-spheres to represent grains. Simulations with a variety of contact properties have been used to demonstrate the impact of the bond strength to stiffness ratio on the characteristic strength of the model grains, and on the stress dependence of soil elements simulated as an assembly of these grains. For grains with a given strength, the peak stress ratio of an element under triaxial compression is shown to reduce realistically as the mean stress increases. Interestingly, this reduction occurs earlier if the bond stiffness is increased.

1 INTRODUCTION

The Discrete Element Method (DEM) can simulate the behavior of crushable soils. Crushable agglomerates are built up by bonding elementary spheres. Realistic simulations of sand behavior will only be possible, however, if the macroscopic functional characterization of the DEM soils can be related to their microscopic grain characterization.

Data are provided from a series of simulations for agglomerates with a variety of bond strengths and contact stiffnesses, following similar work on one-dimensional compression by McDowell & Harireche (2002). Some were single-agglomerate crushing tests, and others followed isotropic and then deviatoric tests on assemblies. The grain properties of interest are the agglomerate crushing strength and stiffness. The corresponding macroscopic parameters for assemblies are the angle of shearing resistance and the locations and slopes of the isotropic compression and critical state lines.

2 DEM OF CRUSHABLE MATERIALS

2.1 *Agglomerates*

Agglomerates were formed following Robertson (2000), being based on a regular assembly of spheres in hexagonal close packing without initial overlap. In order to provide a sand-like variability to the strength and shape of the agglomerates, each elementary sphere was given a probability of existence of only 80% when it was created. These flawed agglomerates contained an average of 46 spheres.

2.2 *Contact model inside agglomerate*

Stiffness, bonding and slip models are included in the constitutive representation of contact points between the elementary spheres. The normal stiffness, K^n, and the shear stiffness, K^s, are computed assuming that the corresponding linear stiffnesses of the two contacting objects act in series. These stiffnesses are here given the same value, K.

The simple contact bond can be envisioned as a pair of elastic springs at a point of glue.The maximum tensile force and the maximum shear force that it can withstand are here made equal to S. This approach follows Robertson and Bolton (2001), McDowell & Harireche (2002) and Cheng, et al. (2003).

Slip occurs between unbounded objects in contact, according to Coulomb friction with a coefficient μ.

2.3 *DEM parameters used*

Table 1 gives the DEM parameters, which model the properties of a typical sand grain as shown in Cheng, et al. (2003). The variety of bond strengths S and contact stiffnesses K used in the simulations are given in Table 2. Agglomerates type 04 are the same as those in Cheng, et al. (2003 & 2004). The influences on mechanical behavior are first examined for

agglomerates with constant $S/K = 2^{*}10^{-6}$ m, indicating the contact displacement when the bond breaks, by comparing types 04, 20 and 25. The effects of varying S/K are discussed using Types 23, 20, 24 which all have $S = 2$N but K varying over a factor of 4.

2.4 *Crushing individual agglomerates*

Randomly-orientated agglomerates were numerically crushed between two smooth and stiff platens under strain-controlled compression. The initial separation of the platens was the same as the size of the agglomerate, which is 1.0 mm. With the variability given to the agglomerates, different peak stresses were obtained from 20 tests.

2.5 *Assembling agglomerates for element tests*

The procedure developed by Robertson (2000) and described in Cheng, et al. (2003) was used to create an assembly of randomly oriented agglomerates with random flaws. Approximately 2% of the total number of bonds broke during the sample preparation. The mean stress at equilibrium was 20 kPa.

The cubical arrangement of 389 agglomerates was then compressed to 0.1 MPa by moving one pair of walls progressively together while continuously adjusting the position of the other two pairs of walls to achieve an isotropic stress path. A wall speed of 0.01 m/s was slow enough to eliminate rate effects. The voids ratio was then 2.1.

Table 1. DEM parameters used (common).

Diameter of agglomerate	1.0 mm
Diameter of sphere	0.2 mm
Density of sphere	2650 kg/m^3
Maximum number of spheres in an agglomerate	57
Maximum number of bonds in an agglomerate	228
Normal and shear bond strength	See Table 2
Normal and shear stiffness of each sphere	See Table 2
Frictional coefficient of sphere	0.5
Percentage of spheres removed at random	20%

3 RELATING PARTICLE CHARACTERISTICS TO MACRO BEHAVIOR

3.1 *Constant bond strength-stiffness ratio*

Figure 1 shows a typical result from the crushing tests for three materials having the same ratio of bond strength to contact stiffness of $2^{*}10^{-6}$ m, and with bond strengths of 4N, 2N and 1N respectively. The applied stress σ is defined as platen force divided by the square of the initial diameter of the agglomerate. The initial peaks are due to readjustment of the agglomerates between the platens.

The Weibull distribution can be used to describe the variability in tensile strengths of apparently identical test-pieces of a brittle material, in which the survival probability P_s is a function of normalised maximum stress σ/σ_0 given by

$$P_s = \exp\left[-\left(\frac{\sigma}{\sigma_0}\right)^m\right] \quad (1)$$

where σ_0 is the characteristic stress at which 37% of sample survive and m is the Weibull modulus. McDowell & Bolton (1998) explain that this approach can be used to estimate m for the sets of grains by carrying out a least-squares regression on a log-log plot.

Table 2. Sets of contact stiffness and bond strength used.

	$K = 2$ MN/m	1 MN/m	0.5 MN/m
$S = 4$N	type04 $S/K = 2^{*}10^{-6}$ m $\sigma_0 = 58.3$ MN/m^2 m = 3.1		
2 N	type23 $S/K = 1^{*}10^{-6}$ m $\sigma_0 = 31.9$ MN/m^2 m = 2.6	type20 $S/K = 2^{*}10^{-6}$ m $\sigma_0 = 30.2$ MN/m^2 m = 3.0	type24 $S/K = 4^{*}10^{-6}$ m $\sigma_0 = 29.2$ MN/m^2 m = 3.2
1 N			type25 $S/K = 2^{*}10^{-6}$ m $\sigma_0 = 15.0$ MN/m^2 m = 3.0

Table 2 shows the lists of σ_0 and m obtained for the agglomerates used here.

Figure 2 shows the stress normalized by σ_0 plotted against displacement for the results shown in Figure 1. The characteristic crushing strength σ_0 was recognized as the normalizing parameter for crushable materials by Robertson (2000). The excellent consistency of the three results can be explained by dimensional analysis. A test at speed V on a particular agglomerate structure, comprising spheres of mass M and diameter d, can be influenced only by three dimensionless groups: $[(V/d)\sqrt{(m/K)}]$, $[S/(Kd)]$ and μ. The first is a dynamics group representing test speed in relation to the speed of compression waves. Apart from the stages where kinetic energy is released by breakage, this group has no effect. The second group was held constant in Figure 2, and μ remains constant throughout this investigation.

Isotropic compression was created with 0.05 m/sec of wall movement. Figure 3 shows the voids ratio plotted against the logarithm of the mean stress p normalized by σ_0 for batches of the three materials shown in Figure 1, for which $S/(Kd)$ is constant.

The normalized compression curves were effectively identical as explained non-dimensionally and as reported by McDowell & Harireche (2002). The compression curves showed only a small decrease of voids ratio until $p/\sigma_0 \approx 0.1$. They achieved maximum curvature at about $p/\sigma_0 \approx 0.2$. Immediately after this the curves became almost straight "normal compression lines" with a gradient $\lambda. = 0.45$, consistent with the concept of fractal crushing. For $p/\sigma_0 > 1$, most bonds had broken, and slope λ reduced to about 0.2, consistent with the concept of comminution limit.

Figure 4 portrays the peak angle of shearing resistance in triaxial compression tests for the same three families of agglomerates. The peak angle was

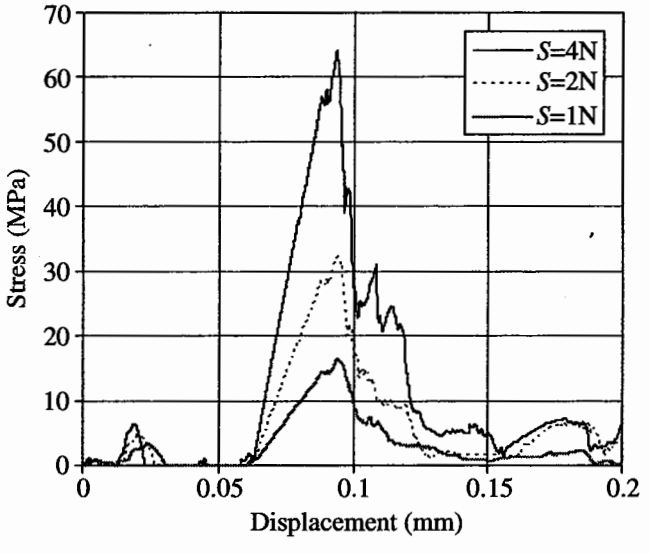

Figure 1. Effect of bond strength on stress versus displacement.

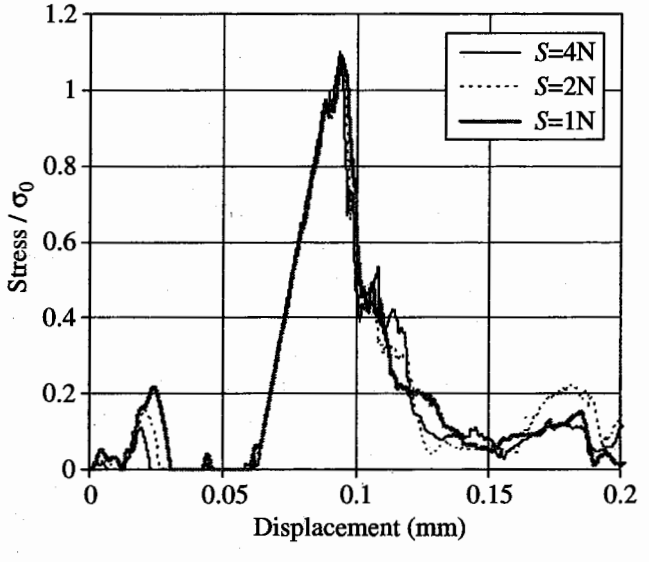

Figure 2. Normalized stress – displacement behavior for agglomerates with various S but unique $S/(Kd)$.

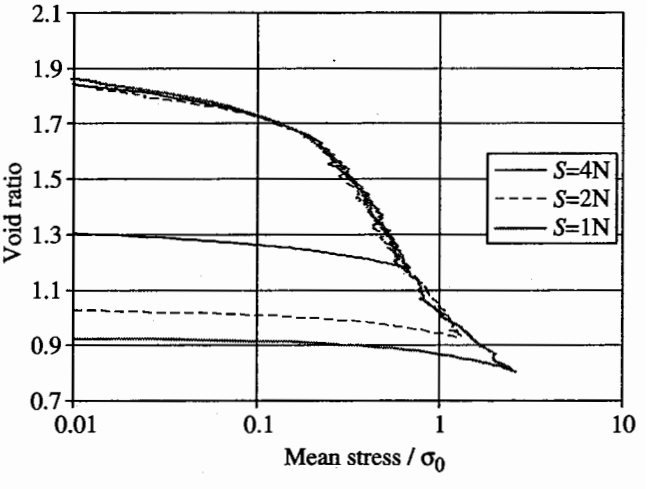

Figure 3. Normalized isotropic compression curves.

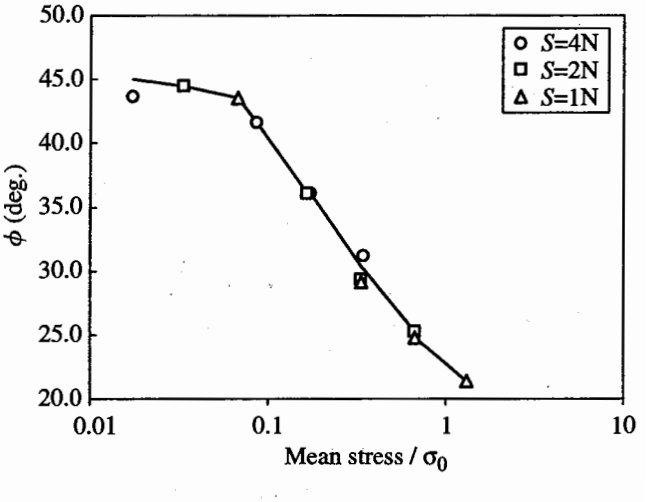

Figure 4. Peak stress ratio versus normalised mean stress.

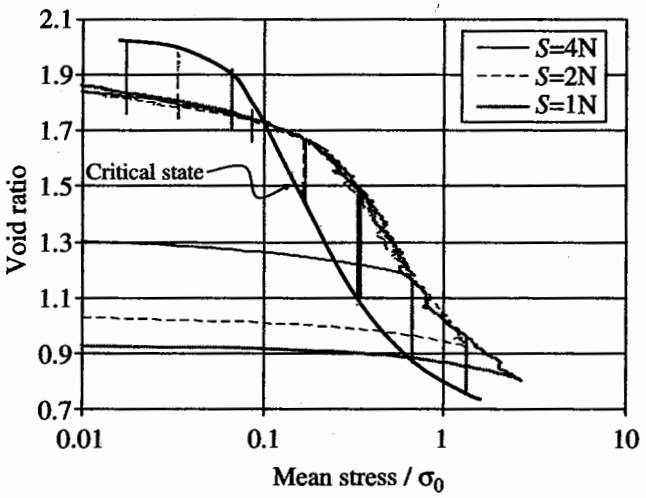

Figure 5. Normalized critical state line.

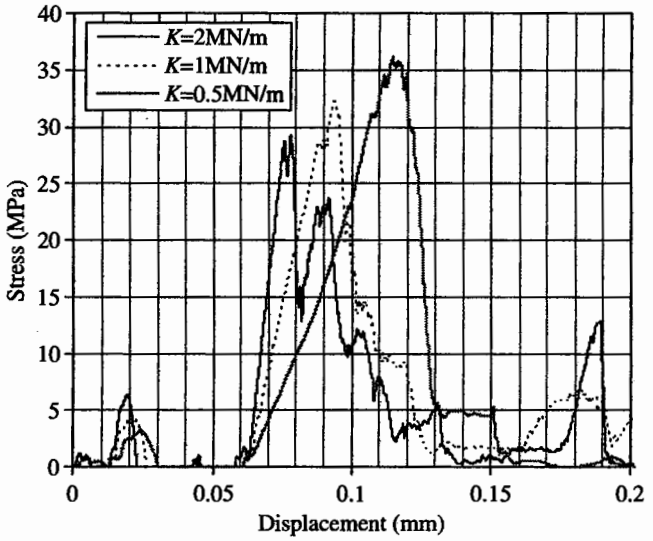

Figure 6. Effect of S/K on single agglomerate crushing.

characterized using the Mohr-Coulomb criterion:

$$\phi = \sin^{-1}[(\sigma_1-\sigma_3)/(\sigma_1+\sigma_3)] \quad (2)$$

The stress level dependency of ϕ is normalized when plotted against the logarithm of the mean stress divided by the characteristic crushing strength, as pointed out experimentally by Bolton (1986) and by McDowell & Bolton (1998).

Figure 5 shows the critical state line for the three agglomerates on a plot of voids ratio versus the normalized mean stress. The critical state line exists about one third unit of natural logarithms inside the fully developed normal compression line, just as Critical State Soil Mechanics suggests.

3.2 *Effect of contact stiffness*

Figure 6 shows results from the crushing tests for three agglomerates having the same bond strength of 2N,

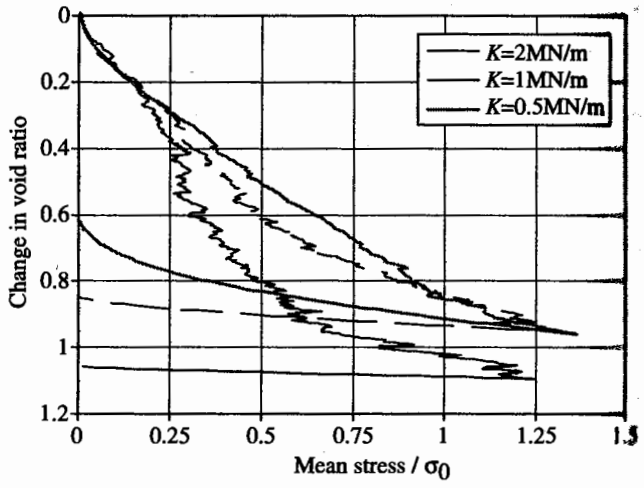

Figure 7. Effect of S/K on isotropic compression.

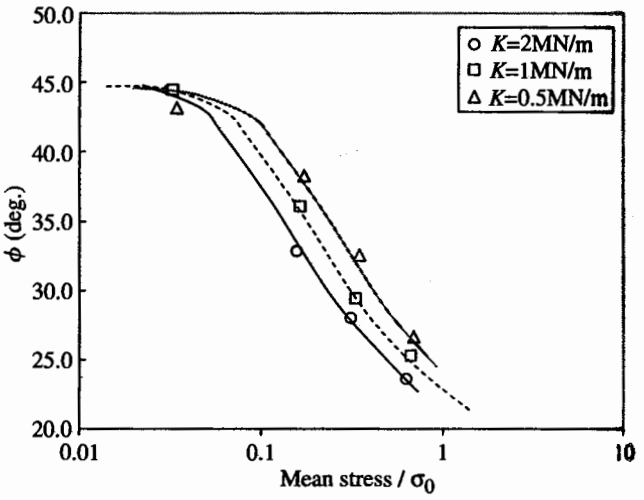

Figure 8. Effect of S/K on curves of peak ϕ versus log p/σ_0.

but with contact stiffnesses K of 2, 1 and 0.5 MN/m respectively. So the ratio of bond strength to contact stiffness varied from $1*10^{-6}$ to $4*10^{-6}$ m.

Figure 7 shows the voids ratio change during isotropic compression plotted against p/σ_0 for assemblies of the three materials represented in Figure 6. All materials gave a slope de/dp of 0.4 at the start of compression, and 0.25 at the end. The intermediate region was dependent on the contact stiffness. As the contact stiffness increased, there was an earlier initiation of increased compressibility, and a greater degree of compression overall. All materials suffered 4% bond breakage during the compression.

Figure 8 shows ϕ versus p/σ_0 for assemblies of the three agglomerates shown in Figure 6. As contact stiffness decreases, the peak angle of shearing resistance increases. As the stiffness of agglomerates decreases, their shape will change more easily, so their coordination number will rise, and contact forces will be dispersed more democratically. Therefore the crushing of agglomerates within the assembly is delayed.

As the result, increasing *S/(Kd)* by reducing *K* delays the effects of breakage, as shown in Figures 7 & 8.

4 CONCLUSIONS

Agglomerates of spheres sharing the same bond strength to stiffness ratio show the same behavior under static loading when stress is normalized by bond strength. The same is true for assemblies of agglomerates, in respect of the reduction of voids ratio following the onset of breakage, both in virgin isotropic compression and ultimate critical states. Increasing the stiffness relative to the bond strength causes earlier onset of breakage in the assembly, increased compressibility, and reduced shear strength.

REFERENCES

Bolton, M. D. (1986). The strength and dilatancy of sands. Géotechnique 36, No. 1, 65–78.

Cheng, Y. P., Nakata, Y. & Bolton, M. D. (2003). Distinct element simulation of crushable soil. *Geotechnique 53, No. 7, 633-641.*

Cheng, Y. P., Bolton, M. D. & Nakata, Y. (2004). Crushing and plastic deformation of soils simulated using dem. *Geotechnique 54, No.1, -.*

McDowell, G. R., Bolton, M. D. & Robertson, D. (1996). The fractal crushing of granular materials. *Int. J. Mech. Phys. Solids* **44**, 2079–2102.

McDowell, G. R. & Bolton, M. D. (1998). On the micromechanics of crushable aggregates. *Géotechnique* **48**, No. 5, 667–679.

McDowell, G. R. & Harireche, O. (2002). Discrete element modelling of soil particle fracture. Technical note. *Geotechnique* **52**, No. 2, 131–135.

Robertson, D. (2000). *Computer simulations of crushable aggregates*. Ph.D. dissertation, Cambridge University.

Robertson, D. & Bolton, M. D. (2001). DEM simulations of crushable grains and soils. Powders and Grains 2001, Kishino (ed.), 623–626.